

Experimental procedures:

Cell Culture

MCF7 cells were grown in RPMI + 10% fetal bovine serum (FBS) supplemented with selective antibiotics (400 µg/ml G418, 5 µg/ml blasticidin, and 0.5 µg/ml puromycin) when needed. The MCF7 and RPE1 p53 reporter cell lines have been previously described (13, 23, and 24). To create the dual p53/MDMX reporter cell line, the MCF7 p53 reporter cell line was transfected with a pInducer20 plasmid containing the mKate2-*MDMX* sequence. Cells were subjected to limiting dilution to obtain single clones and screened for mKate2 expression.

Antibodies and Reagents

Antibodies were used against MDMX (IHC-00108, Bethyl lab and 8C6, Millipore), Mdm2 (SMP14, Santa Cruz), p53 (DO1 and FL-393, Santa Cruz), p21 (Ab1, Calbiochem), H2A.X-P(Ser139) (JBW301, Millipore), Chk1 (2345, Cell Signaling), Chk1-P(Ser317) (2345, Cell Signaling), Chk2 (2662, Cell Signaling), Chk2-P(Thr68) (2661, Cell Signaling), PUMA (4976, Cell Signaling), Akt (2920, Cell Signaling), Akt-P(S473P) (5012, Cell Signaling), and Actin (A3854, Sigma). Neocarzinostatin, protease and phosphatase inhibitors were from Sigma; DharmaFect I from Dharmacon and small interfering RNAs targeting MDMX (sequences: AGCCCTCTCTATGATATGCTA and GACCACGAGACGGGAACATTA) and Mdm2 (sequences: CAGGCAAATGTGCAATACCAA and CTCTGTCTTAAATGAGAAGTA) from Qiagen were used for MDMX and Mdm2 depletion respectively. In both cases, two siRNAs provided similar results. Neocarzinostatin and doxycycline concentrations are both 100 ng/ml. For all MDMX knockdowns, 5nM of siRNA was used unless stated otherwise.

Western Blot Analysis

Cells were harvested with RIPA buffer (05-01) (Cold Spring Harbor Protocols) containing protease and phosphatase inhibitors. Equal protein amounts were separated by electrophoreses on 4%–12% Bis-Tris gradient gels (Invitrogen) and transferred to PVDF membranes by electroblotting. Membranes were blocked with either 5% BSA or nonfat dried milk, incubated with primary antibody overnight, washed, then incubated with secondary antibody for 1 hr followed by additional wash. Protein levels were quantified with either chemoluminescence (ECL plus, Amersham) or infrared fluorescence (ODYSSEY, LI-COR).

Live-Cell Microscopy

Cells were grown in RPMI without phenol red and riboflavin + 10% FBS in poly-D-lysine coated glass-bottom plates (MatTek Corporation) for two days before imaging. We used Nikon Eclipse TE-2000 inverted microscope with a 20× plan apo objective (NA 0.75) with a Hammamatsu Orca ER camera. The microscope was equipped with an

environmental chamber controlling temperature, atmosphere (5% CO₂), and humidity. Images were acquired every 30 min for 24-72 hr controlled by MetaMorph Software (Molecular Devices). Image analysis was done with ImageJ (NIH) and Matlab (MathWorks).

Immunofluorescence

Cells were grown on glass-bottom plates (MatTek Corporation) coated with poly-D-lysine and fixed with 4% paraformaldehyde. Cells were permeabilized in PBS/1% Triton for 5 min, blocked with 2% BSA, incubated with primary antibody overnight, washed, and incubated with secondary antibody coupled to either Alexa488 or Alexa647. After washing, cells were stained with DAPI and embedded in imaging media (20mM Tris-HCl, pH8.0, 2.5% DABCO and 80% Glycerol). Images were acquired with a 20× plan apo objective (NA 0.75) with the appropriate filter sets. Image analysis was done with CellProfiler (25). At least fifty thousand cells were measured per condition.

Cell Viability Assay

Cell viability is measured using CellTiter-Glo Luminescent Cell Viability Assay (Promega) following a standard protocol.

Supplementary Figure Legends

(S1) Distribution of cell cycle lengths

Cell cycle lengths of individual cells (MCF7: A, and RPE1: B) were recorded using time-lapse microscopy as the time interval between two mitotic events ($n > 100$ cells).

(S2) Single cells show biphasic p53 dynamics after MDMX depletion in RPE1 cells

(A, B and C) Time-lapse microscopy images of RPE1 cells expressing p53-mYFP after transfection with scrambled (A) or MDMX (B) siRNAs or after NCS treatment.

Abundance of p53 in individual cells tracked as fluorescence p53-mYFP. Dashed lines indicate cell division. p53-mYFP dynamics in MDMX depleted cells are classified into phase I (first post-mitotic pulse) and phase II (low amplitude oscillations). Double strand breaks (DSBs) were introduced by NCS.

(D) Heat map of p53-mYFP levels after MDMX depletion. Red squares indicate the time of cell division.

(E) The mean relative widths (measured by full width at half maximum) of p53 pulses in control cells and MDMX KD cells ($n > 90$ p53 pulses; error bars indicate S.D..)

(F) Amplitudes of p53 pulses in control cells and MDMX KD cells ($n > 90$ p53 pulses; error bars indicate S.D.; * $P < 10^{-2}$, *** $P < 10^{-22}$; P -values obtained by Student's two-sample unequal variance t-Test, with a two-tailed distribution).

(G) Periods of p53 oscillations in MDMX knockdown [II] and NCS-treated cells are measured by autocorrelation.

(H) The mean relative amplitude of p53 oscillations in MDMX knockdown [II] and NCS-treated cells are shown ($n > 90$ pulses; error bars indicate S.D.; *** $P < 10^{-24}$; P -values obtained by Student's two-sample unequal variance t-Test, with a two-tailed distribution).

(S3) p53 does not show oscillations after Mdm2 knockdown

Time-lapse microscopy images of MCF7 cells expressing p53-mCerulean after transfection with scrambled (A and B) or Mdm2 (C and D) siRNAs. Abundances of p53-mCerulean of twenty cells (A and C) and of individual cells (B and D) are shown.

Triangles with dashed lines indicate cell division. Mdm2 depleted cells show a p53 pulse after division followed by an increase in p53. (E) Western blot analysis showed the levels of Mdm2, p53 and actin during the three-day period after Mdm2 siRNA transfection. The reduced efficacy of Mdm2 siRNA at 72 hr is likely due to stabilization of p53.

(S4) MDMX suppresses p53 oscillations after DNA damage

(A) MDMX is degraded after γ -irradiation. Abundance of p53, Mdm2 and MDMX protein after γ -irradiation analyzed by western blot. (B) Higher level of MDMX suppresses DSB-induced p53 oscillations. Percentages of cells showing 1st, 2nd and 3rd p53 pulses after NCS treatment alone or with 12 hr prior doxycycline treatment to induce mKate2-MDMX expression.

(S5) p21 accumulation after MDMX depletion is dependent on p53

Abundance of p21 protein after MDMX knockdown analyzed with western blot in wild-type (left) and p53sh (right) cells.

(S6) DNA damage induced accumulation of p53 is higher in MDMX depleted cells during phase I but not phase II

The maximum abundance of p53 in control and MDMX depleted cells when DNA damage applied during phase I (S6A) or phase II (S6B) of MDMX suppression (n =100 cells; error bars indicate the S.D.; ** $P < 10^{-11}$; phase II p53 abundances of both treatments are not statistically significantly different $P = 0.99$; P -values obtained by Student's two-sample unequal variance t-Test, with a two-tailed distribution).

(S7) Schedule-dependent interactions between MDMX suppression and multiple drugs

MCF7 (A) and RPE1 (B) cells were transfected with scrambled or MDMX siRNA followed by drug treatments at 12 hr (phase I) or 48 hr (phase II) after transfection. Drugs used are 4NQO (200 nM), doxorubicin (10 μ M), camptothecin (4 μ M) and actinomycin D (200 nM). Relative cell survival rates were measured using cell viability assay 24 hr after drug treatments (n = 3 biological repeats; error bars indicate the S.D.).

(S8) Cells in phase II of MDMX suppression showed stronger pro-survival signals after DNA damage

Cells either transfected with scrambled (left) or MDMX siRNAs (right) were treatment with ultraviolet radiation (16 J/m²) 48 hr after transfection. Time points after ultraviolet irradiation (0-24 hr) were prepared for western blot analysis probing abundances of p53, Mdm2, MDMX, PUMA (pro-apoptotic marker), p21 (pro-survival marker), Akt, phospho-Akt (S473P) (pro-survival marker) and actin proteins.

Reference:

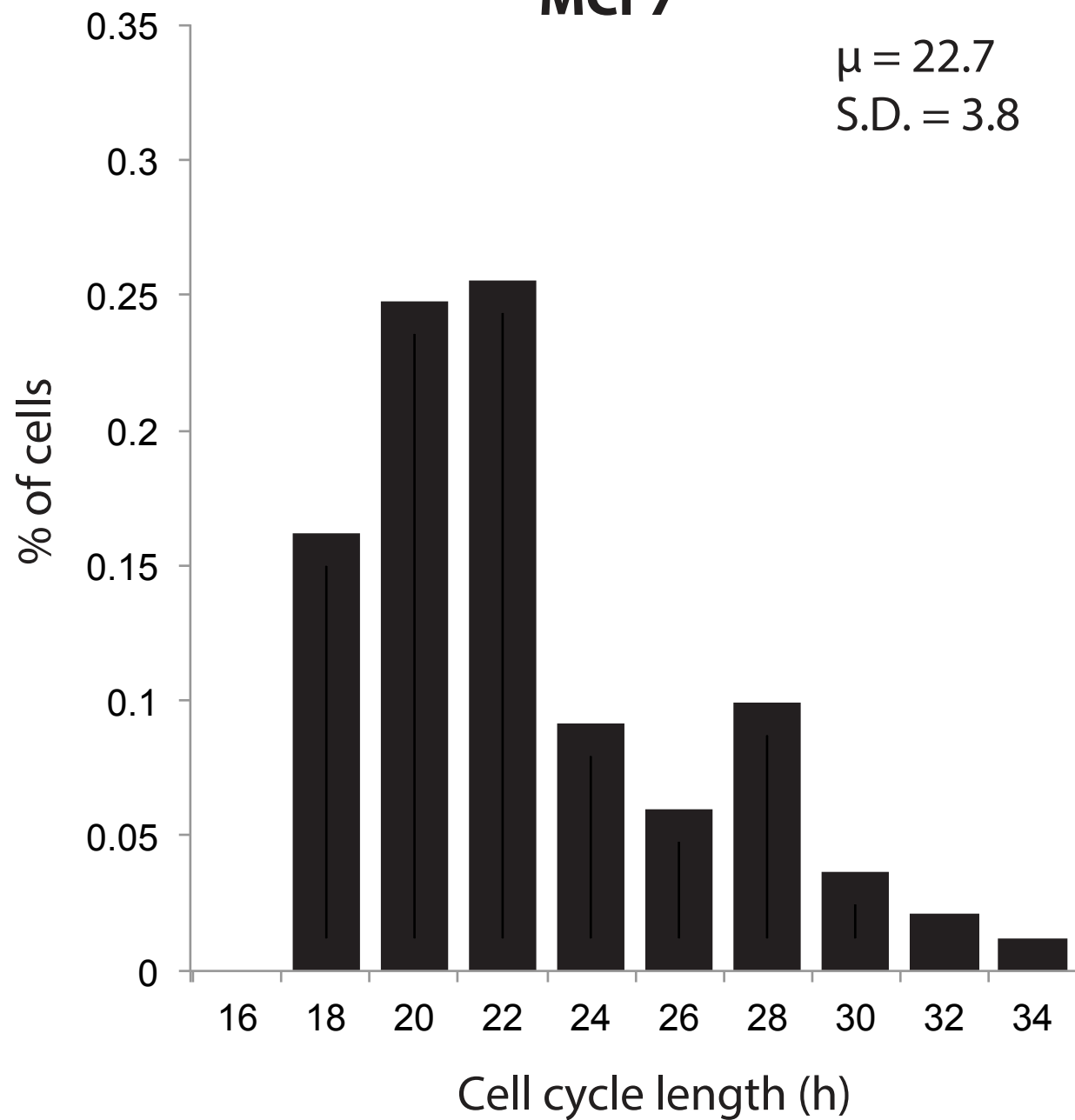
23. A. Loewer, K. Karanam, C. Mock, G. Lahav, The p53 response in single cells is linearly correlated to the number of DNA breaks without a distinct threshold. *BMC Biol.* **11**, 114 (2013).
24. G. Gaglia, Y. Guan, J. V. Shah, G. Lahav, Activation and control of p53 tetramerization in individual living cells. *Proc. Natl. Acad. Sci. U.S.A.* **110**, 15497–15501 (2013).
25. A. E. Carpenter *et al.*, CellProfiler: image analysis software for identifying and quantifying cell phenotypes. *Genome Biol.* **7**, R100 (2006).

S1

A

MCF7

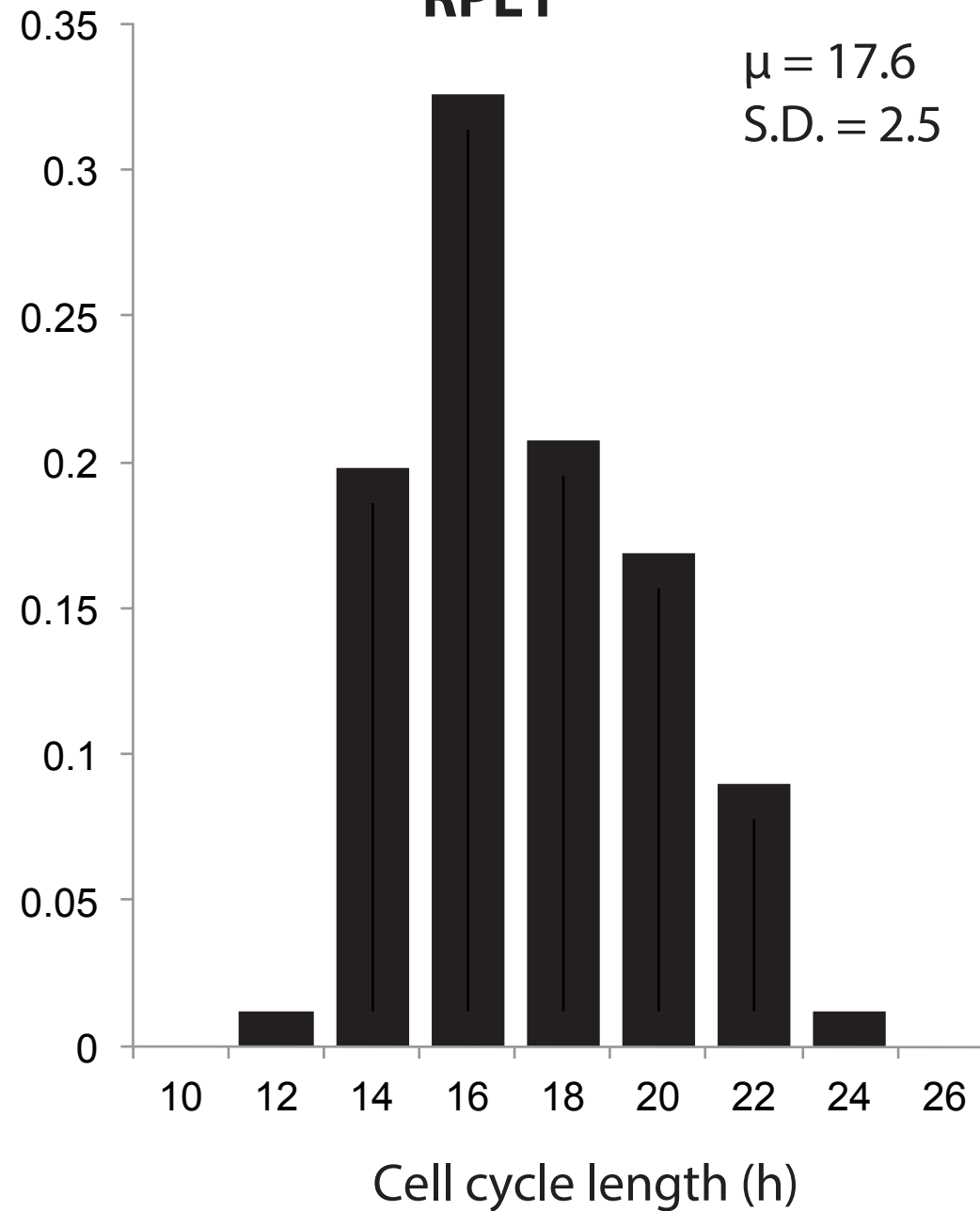
$\mu = 22.7$
S.D. = 3.8



B

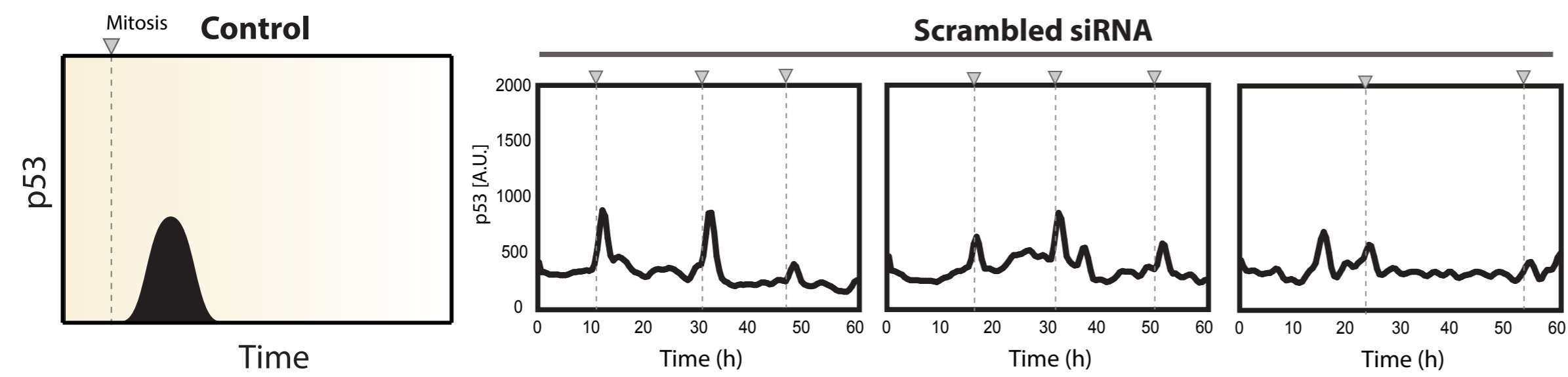
RPE1

$\mu = 17.6$
S.D. = 2.5

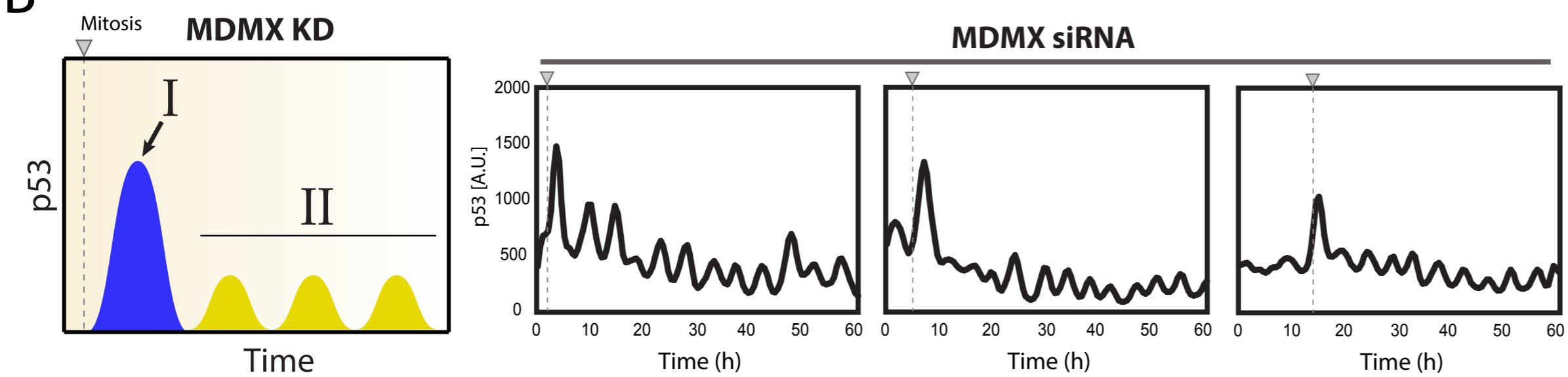


S2

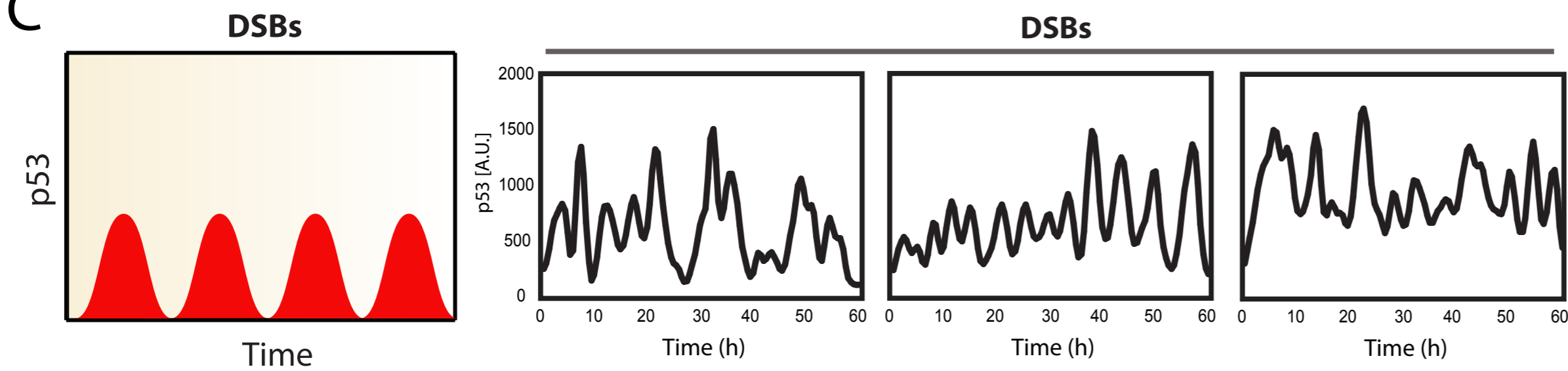
A



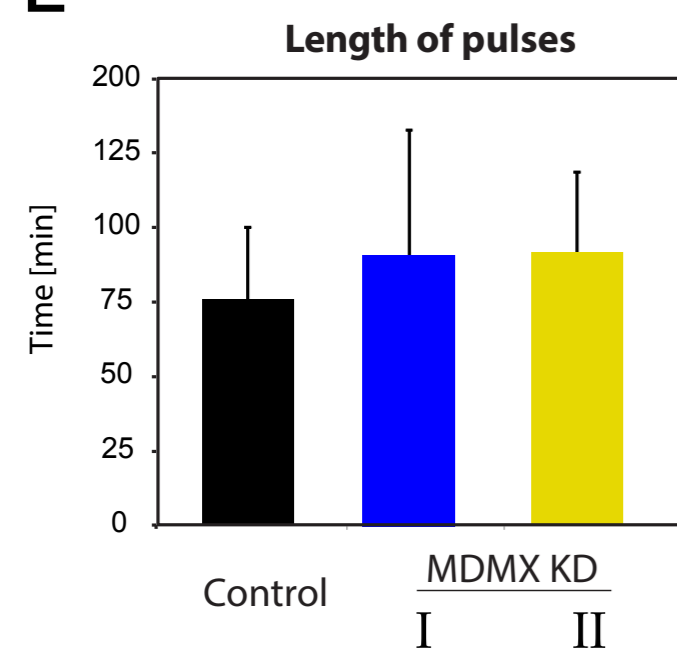
B



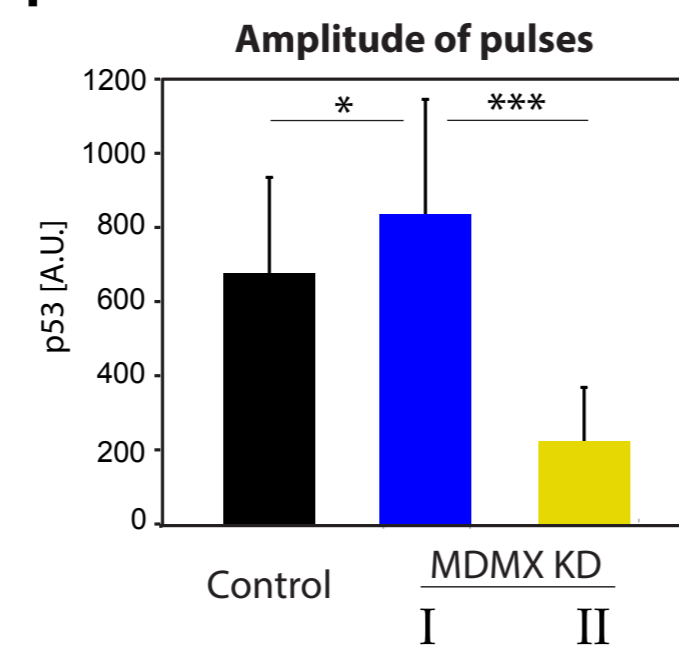
C



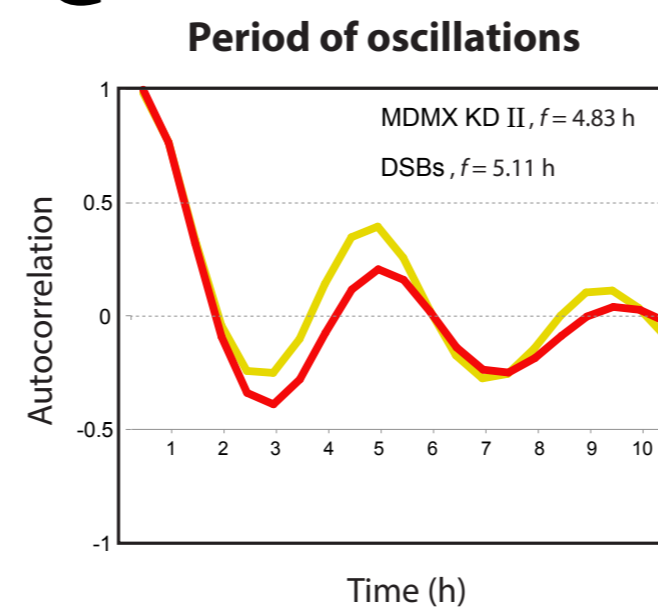
E



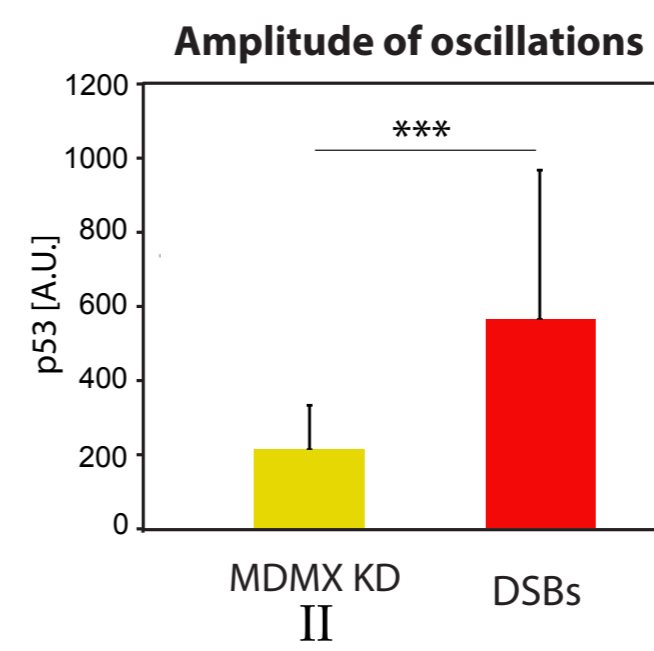
F



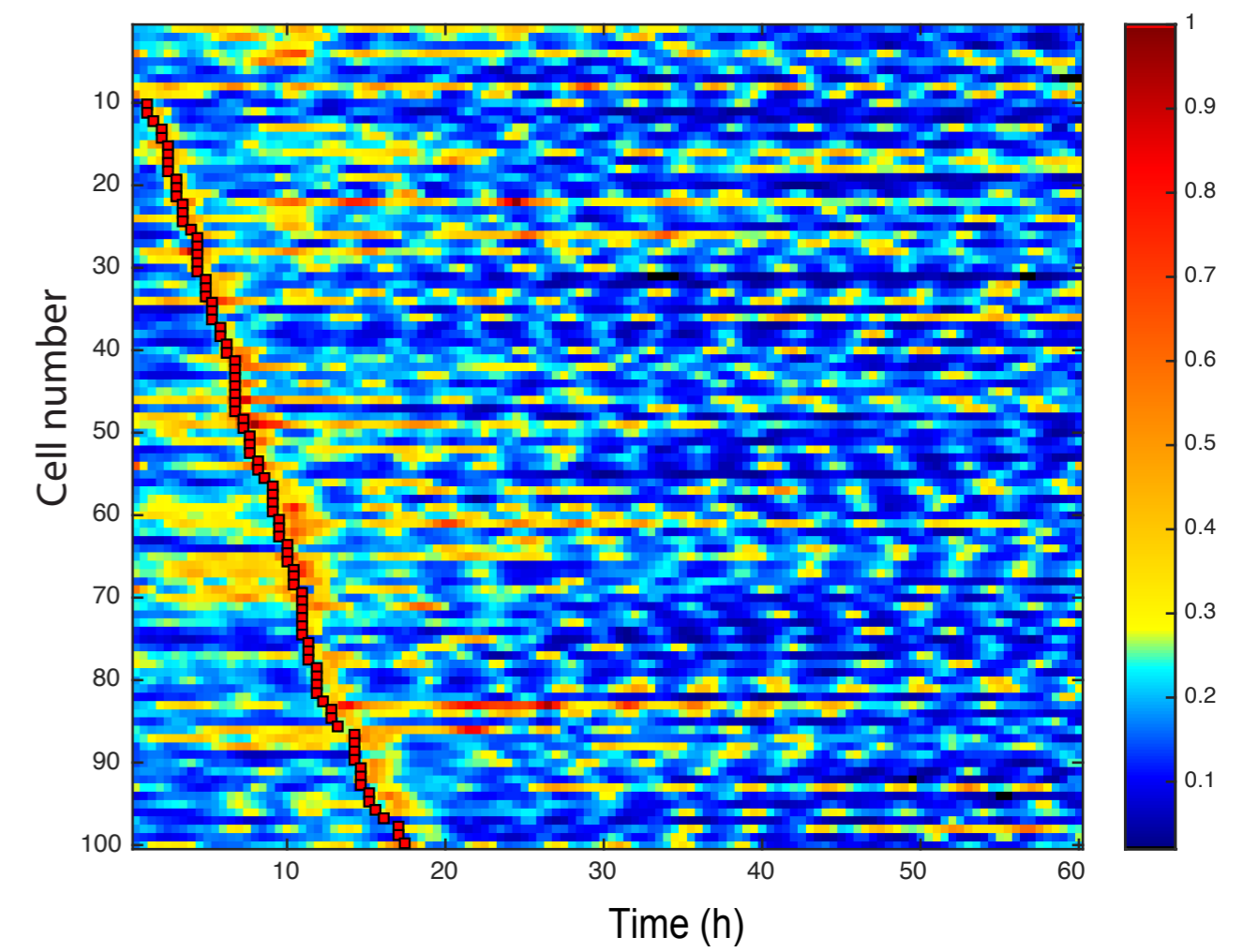
G



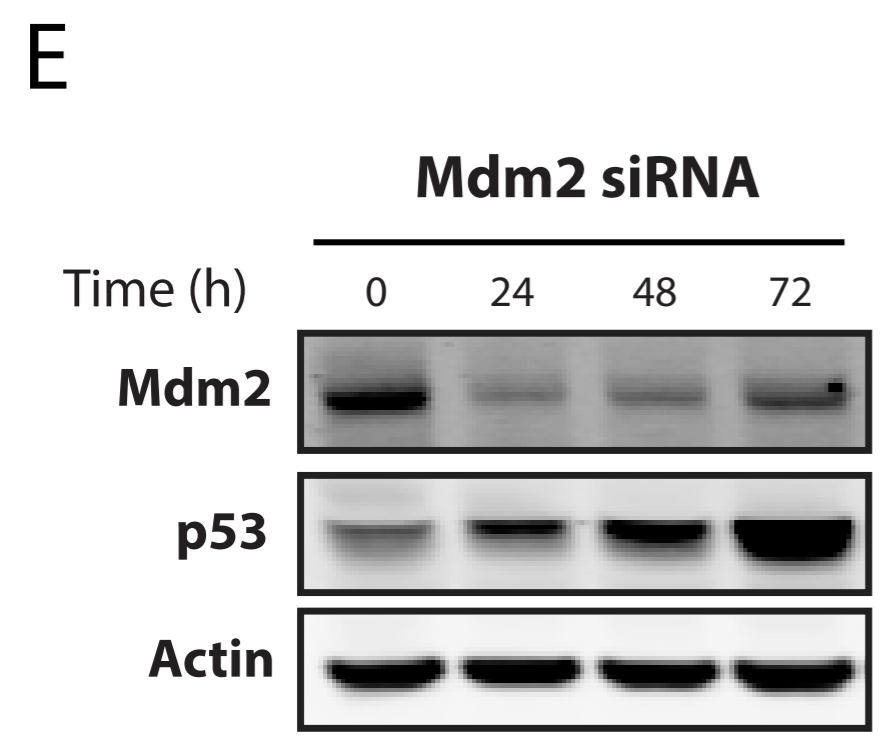
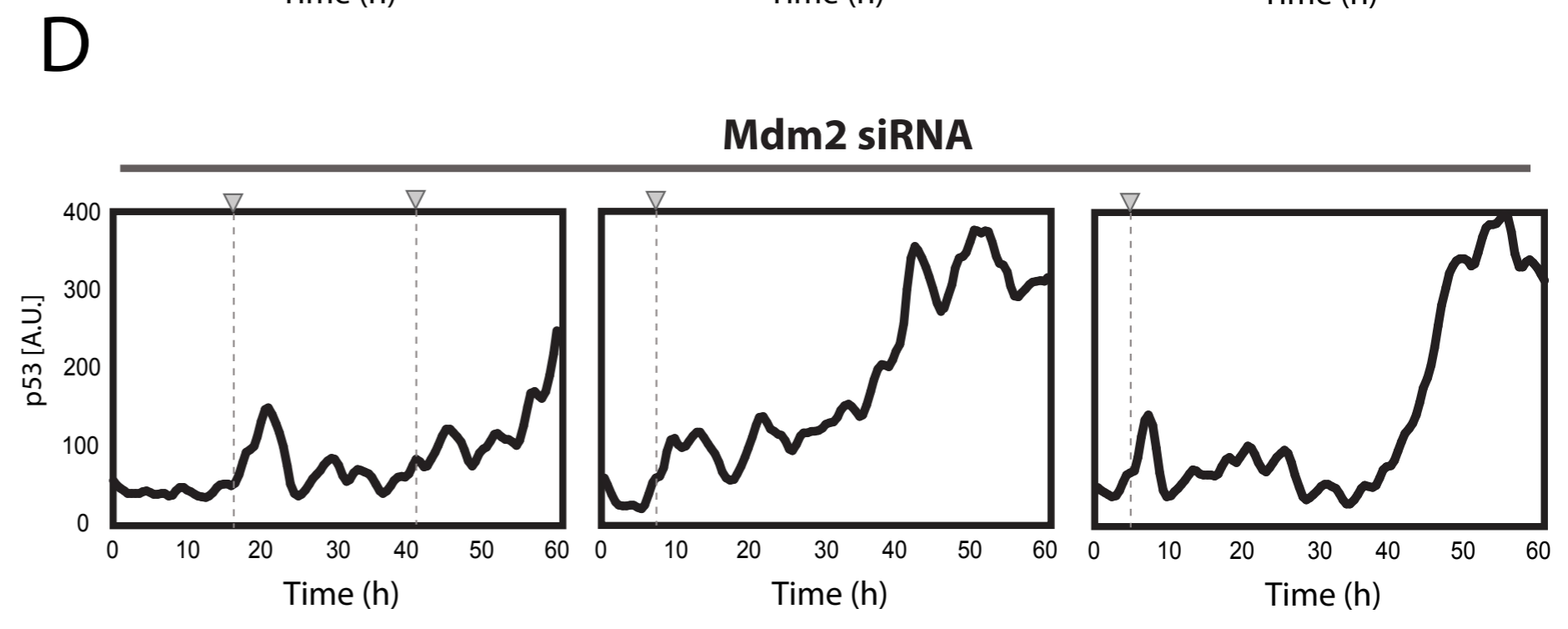
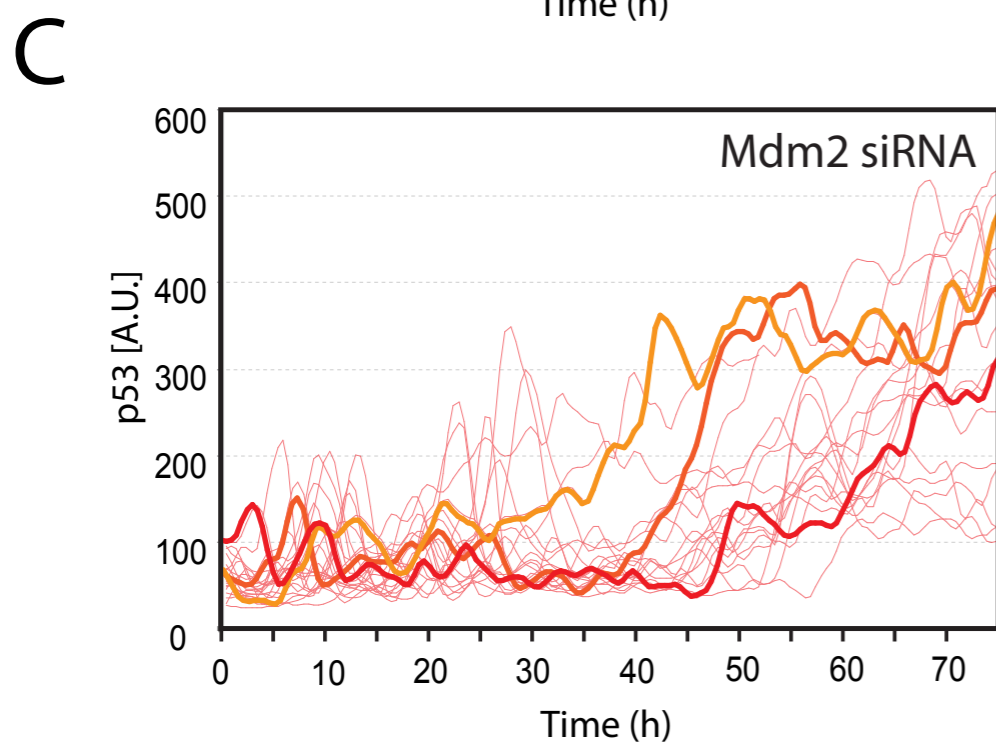
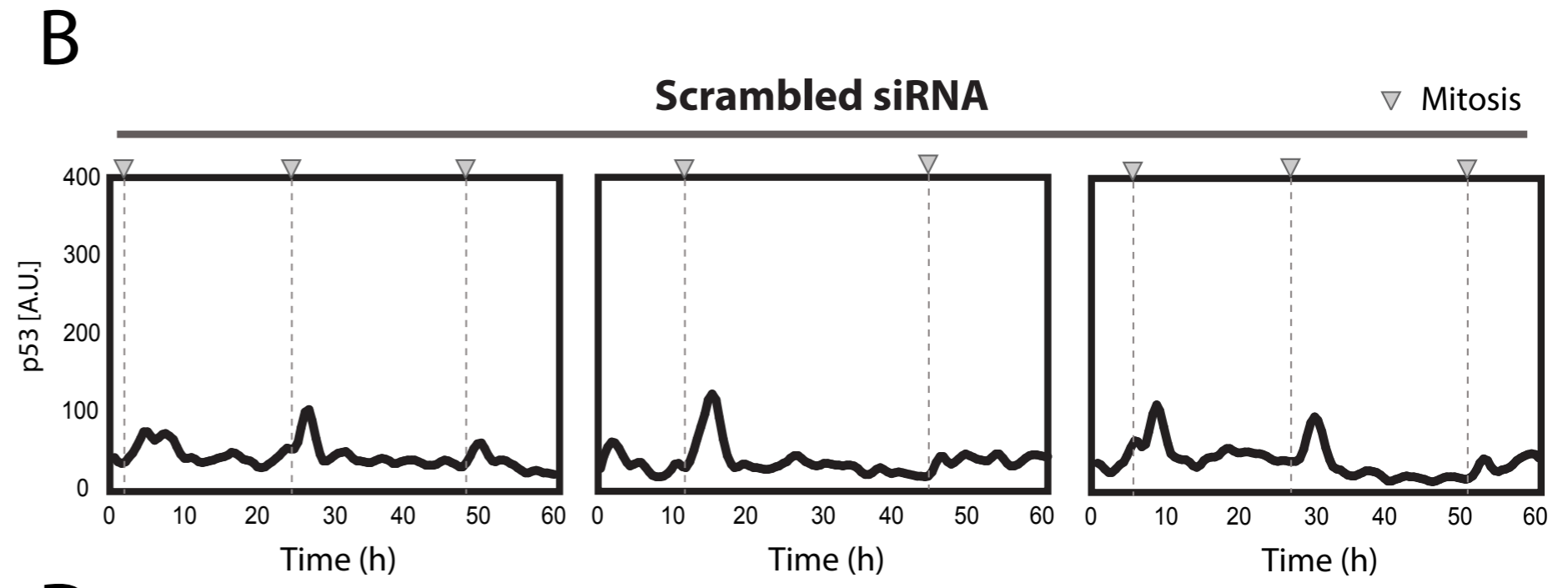
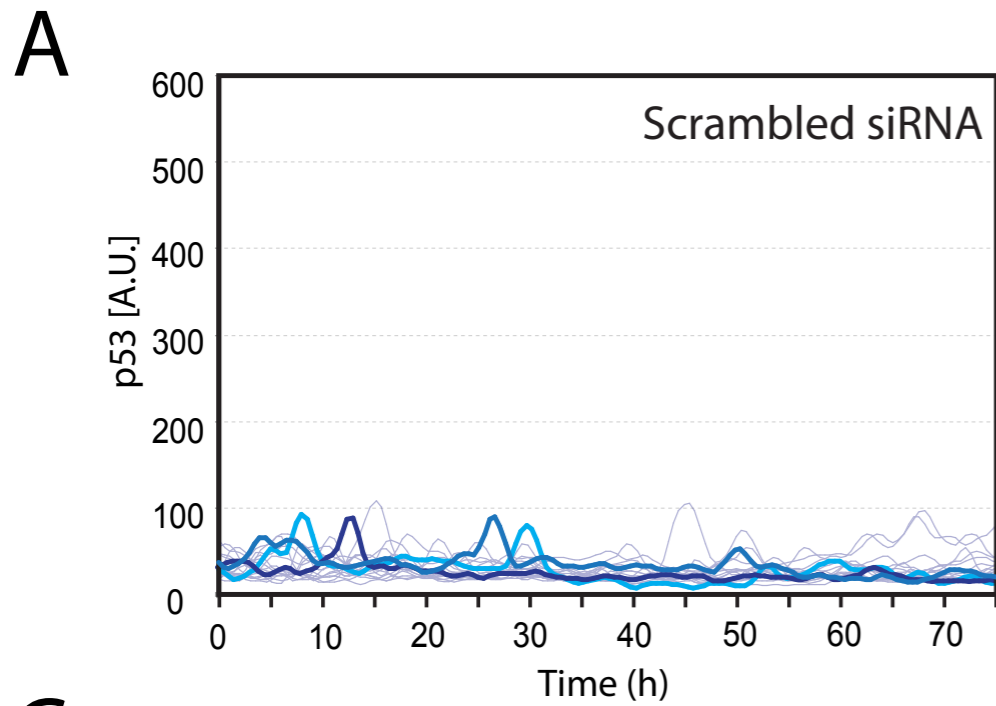
H



D

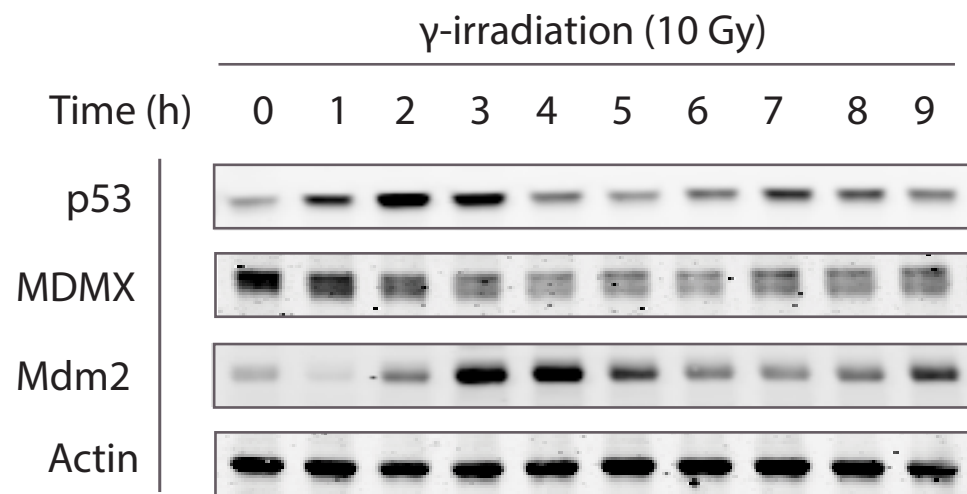


S3

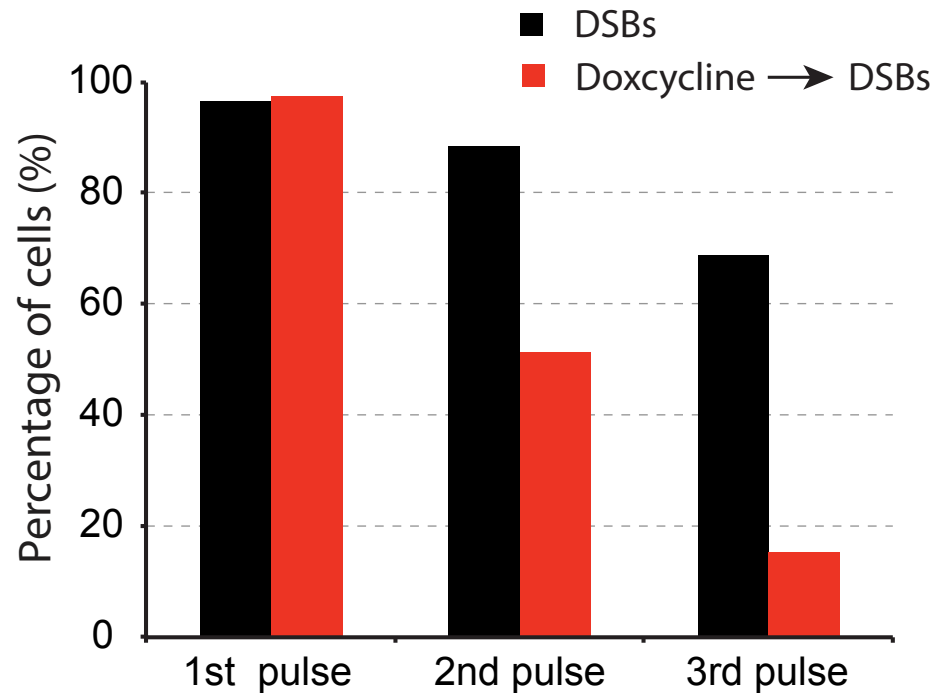


S4

A



B

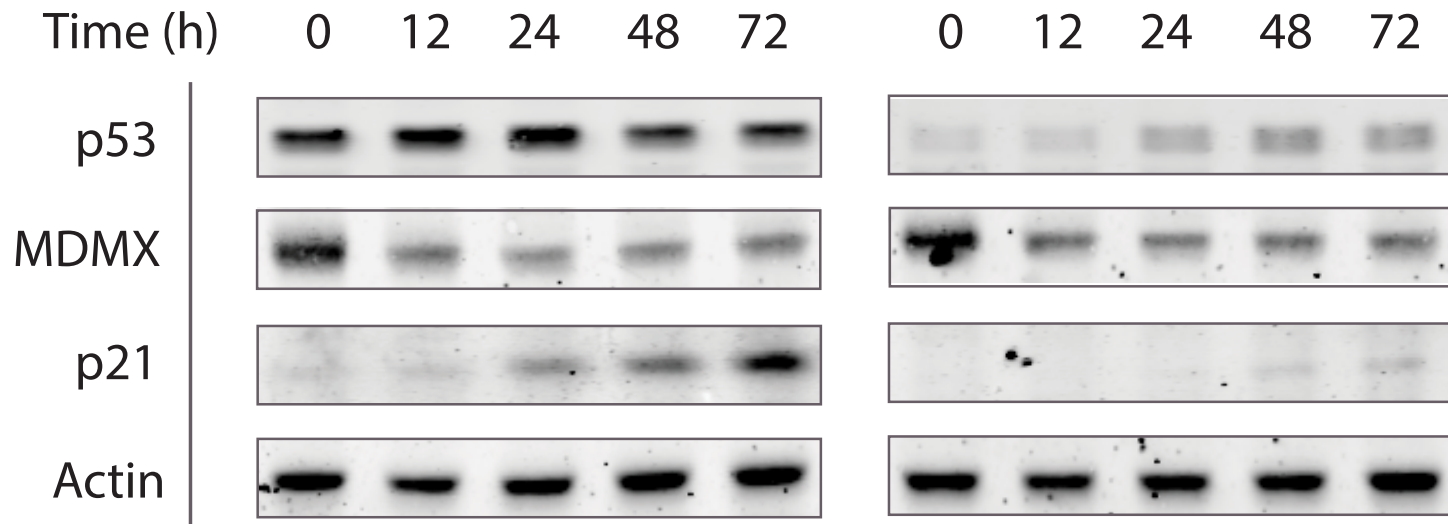


S5

MDMX siRNA

WT

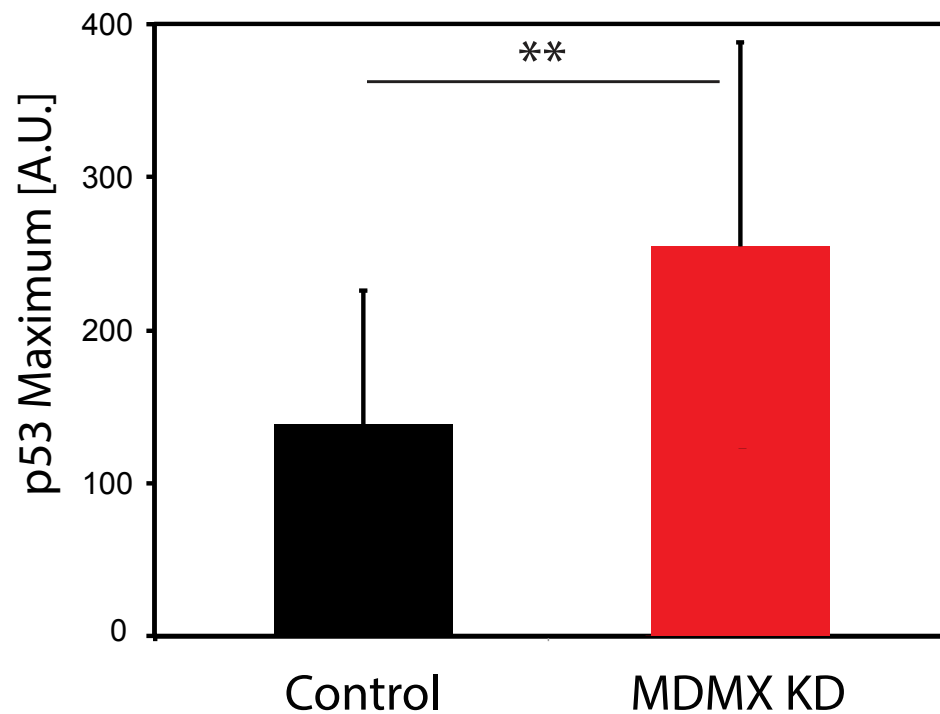
p53sh



S6

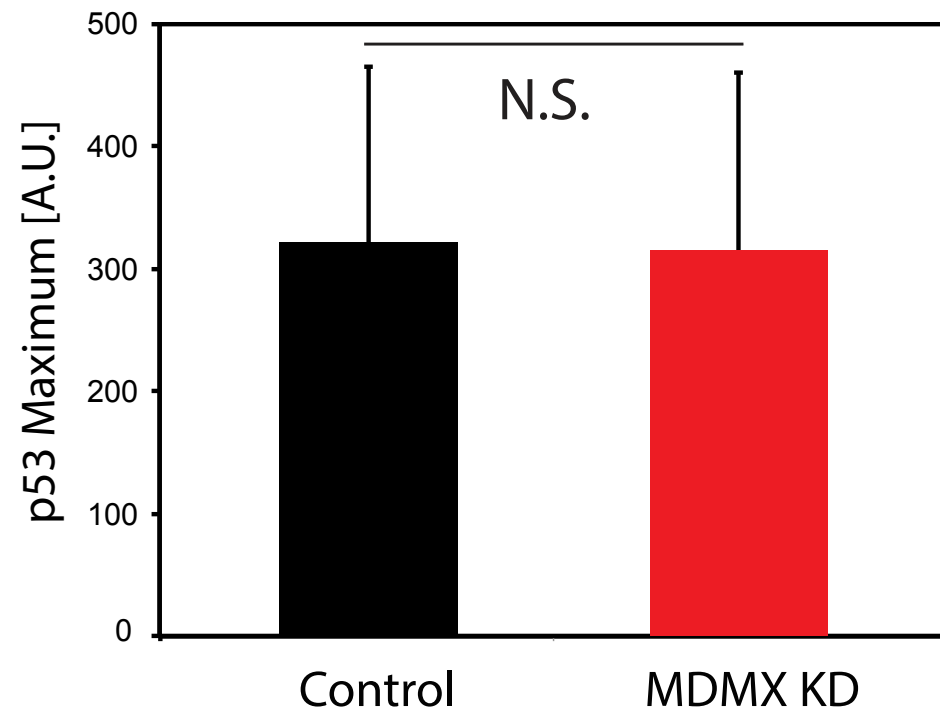
A

DNA damage at phase I



B

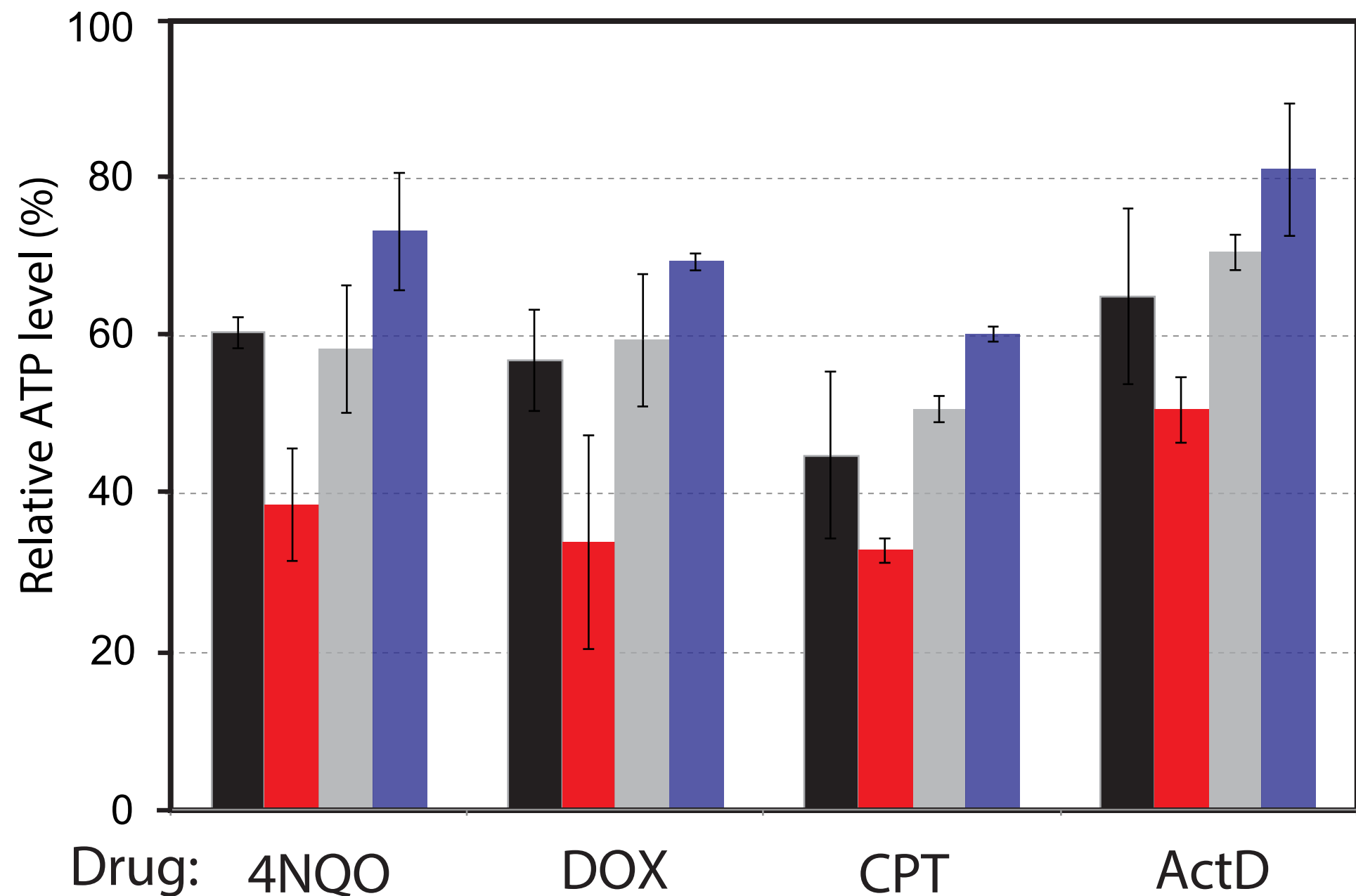
DNA damage at phase II



S7

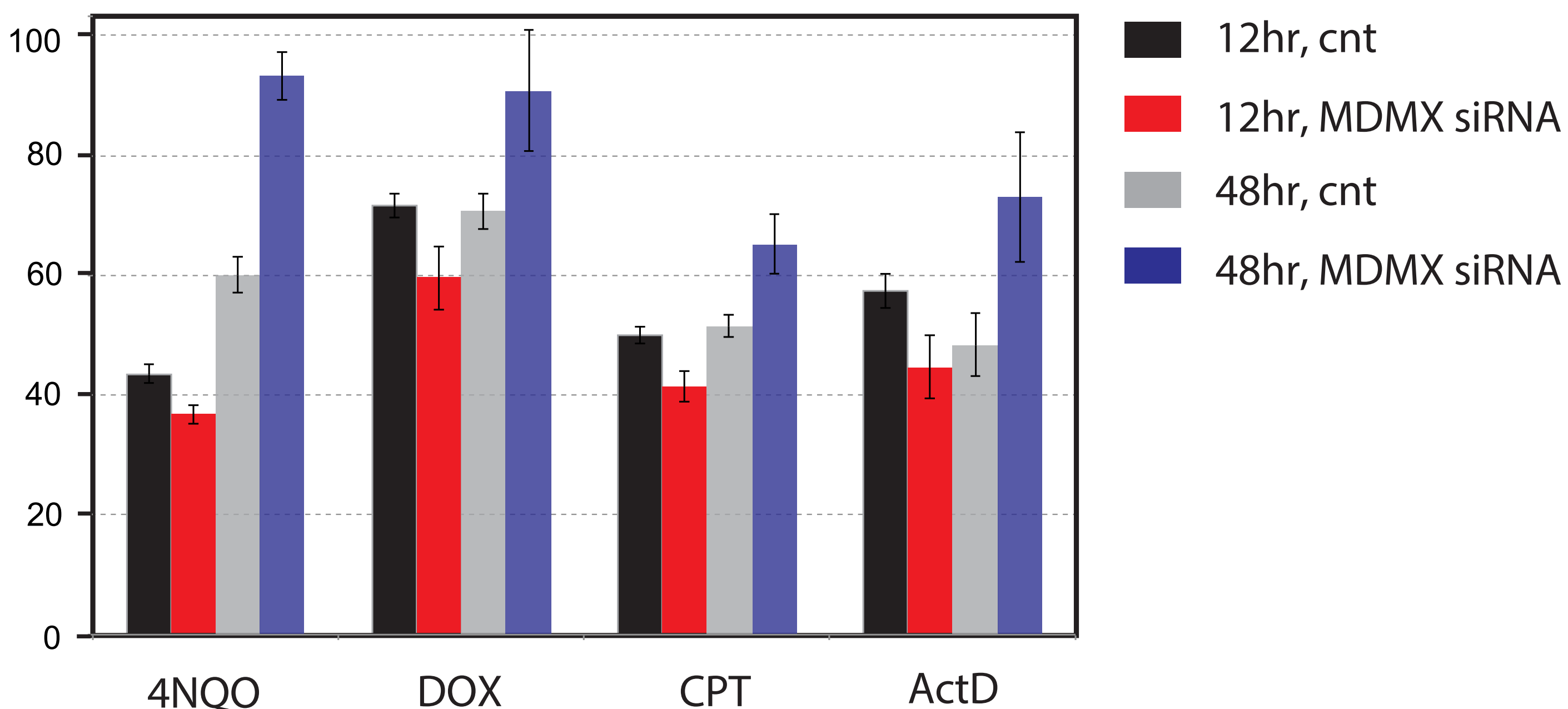
A

Relative survival after drug treatments (MCF7)



B

Relative survival after drug treatments (RPE)



- 12hr, cnt
- 12hr, MDMX siRNA
- 48hr, cnt
- 48hr, MDMX siRNA

